Cancer Science
Japanese Cancer Association JCA Open Access

Stathmin1 regulates p27 expression, proliferation and drug resistance, resulting in poor clinical prognosis in cholangiocarcinoma

Akira Watanabe,[1] Hideki Suzuki,[1] Takehiko Yokobori,[1] Mariko Tsukagoshi,[1] Bolag Altan,[1] Norio Kubo,[1] Shigemasa Suzuki,[1] Kenichiro Araki,[1] Satoshi Wada,[1] Kenji Kashiwabara,[2] Yasuo Hosouchi[3] and Hiroyuki Kuwano[1]

[1]Department of General Surgical Science, Gunma University Graduate School of Medicine, Gunma; [2]Pathological Department, Gunma Prefecture Saiseikai-Maebashi Hospital, Gunma; [3]Department of Surgery and Laparoscopic Surgery, Gunma Prefecture Saiseikai-Maebashi Hospital, Gunma, Japan

Key words

Cancer progression, drug resistance, extrahepatic cholangiocarcinoma, p27, stathmin1

Correspondence

Akira Watanabe, Department of General Surgical Science (Surgery I), Gunma University Graduate School of Medicine, 3-39-22 Showa-machi, Maebashi, Gunma 371-8511, Japan.

Tel: +81 2 7220 8224; Fax: +81 2 7220 8230;
E-mail: akira_watanabe@gunma-u.ac.jp

Funding information
None declared.

Received February 9, 2014; Revised April 3, 2014; Accepted April 6, 2014

*Cancer Sci*105 (2014) 690–696

doi: 10.1111/cas.12417

Patients with extrahepatic cholangiocarcinoma (EHCC) have a poor prognosis; postoperative survival depends on cancer progression and therapeutic resistance. The mechanism of EHCC progression needs to be clarified to identify ways to improve disease prognosis. Stathmin1 (STMN1) is a major cytosolic phosphoprotein that regulates microtubule dynamics and is associated with malignant phenotypes and chemoresistance in various cancers. Recently, STMN1 was reported to interact with p27, an inhibitor of cyclin-dependent kinase complexes. Eighty EHCC cases were studied using immunohistochemistry and clinical pathology to determine the correlation between STMN1 and p27 expression; RNA interference to analyze the function of STMN1 in an EHCC cell line was also used. Cytoplasmic STMN1 expression correlated with venous invasion ($P = 0.0021$) and nuclear p27 underexpression ($P = 0.0011$). Patients in the high-STMN1-expression group were associated with shorter recurrence-free survival and overall survival than those in the low-expression group. An *in vitro* protein-binding assay revealed that cytoplasmic STMN1 bound to p27 in the cytoplasm, but not in the nucleus of EHCC cells. Moreover, p27 accumulated in EHCC cells after STMN1 suppression. STMN1 knockdown inhibited proliferation and increased the sensitivity of EHCC cells to paclitaxel. STMN1 contributes to a poor prognosis and cancer progression in EHCC patients. Understanding the regulation of p27 by STMN1 could provide new insights for overcoming therapeutic resistance in EHCC.

Cholangiocarcinoma is associated with poor prognosis and its incidence and mortality are increasing worldwide.[1] The 5-year survival rate for cholangiocarcinoma is 10–40%.[2] Cholangiocarcinoma is defined as intrahepatic or extrahepatic (EHCC), the latter of which consists of hilar or bile duct tumors. Surgical therapy is the only effective curative treatment for EHCC; postoperative survival is dependent on the existence of invasion and metastasis.[3,4] Therefore, to improve patient prognoses, we must understand the mechanism of cancer progression in EHCC.

Stathmin1 (STMN1) is a major cytosolic phosphoprotein that regulates microtubule dynamics by preventing tubulin polymerization and promoting microtubule destabilization. STMN1 plays an important role in a variety of biological processes, including carcinogenesis. STMN1 is highly expressed in various types of human malignancies and is therefore also known as oncoprotein 18 (OP18). Moreover, STMN1 expression correlates with tumor progression and poor prognosis in the following cancers: breast cancer,[5–7] prostate cancer,[8] gastric cancer,[9,10] hepatocellular carcinoma,[11,12] oral squamous cell carcinoma,[13] colorectal cancer,[14,15] malignant mesothelioma[16] and urothelial carcinoma.[17] Thus, *STMN1* is a fundamental cancer-associated gene and a potential target for diagnosis and treatment. To our knowledge, STMN1 expression in EHCC has not been reported; therefore, we explored the role of STMN1 in EHCC.

STMN1 regulates microtubule metabolism and contributes to tumor progression. Baldassarre *et al.*[18] reported that STMN1 bound to p27 suppressed the function of p27 and enhanced the proliferation of tumor cells. p27 was discovered as an inhibitor of cyclin-dependent kinase (CDK) complexes in TGF (transforming growth factor) β-arrested cells and was classified as a member of the Cip/Kip family of cyclin-dependent kinase inhibitors (CKI).[19] The CKI associate with a broad spectrum of cyclin–CDK complexes to negatively regulate progression through the G1 phase of the cell cycle. More recently, cytoplasmic p27 was shown to play a role in the regulation of cell migration.[20] However, there are still few reports that discuss the relationship of STMN1 and p27 in malignancy, including EHCC. Therefore, we examined the relationship between STMN1 and p27 in EHCC.

The purpose of the present study was to clarify the function of STMN1 in EHCC cell lines *in vitro*, determine the clinical significance of STMN1 in primary EHCC and evaluate the relationship between STMN1 and p27. To this end, we performed immunohistochemistry to evaluate the relationships between STMN1, p27 and clinicopathological factors in clinical EHCC samples. We also examined the *in vitro* effects of

siRNA-mediated STMN1 suppression on the proliferation, chemotherapeutic sensitivity and p27 expression in human EHCC cell lines.

Material and Methods

Patients and samples. Imunohistochemistry was performed on 80 EHCC patients who had undergone curative surgery in our department between 1995 and 2011. Patients ranged in age from 43 to 94 years. Tumor stage was classified according to the seventh tumor–node–metastasis (TNM) classification of the Union for International Cancer Control (UICC).[21] Forty-four (53%) patients received adjuvant therapy following chemotherapy: 11 received UFT (tegafur-uracil; Taiho Pharmaceutical, Tokyo, Japan); nine received Gemcitabine (Eli Lilly and Company, Indianapolis, IN, USA); 21 received S-1 (TS-1; Taiho Pharmaceutical); and three received Gemcitabine+S-1. All patients provided written informed consent, as per institutional guidelines.

Immunohistochemical staining. A 4-μm section was cut from paraffin blocks of EHCC samples. Each section was mounted on a silane-coated glass slide, deparaffinized and soaked for 30 min at room temperature in 0.3% H_2O_2/methanol to block endogenous peroxidases. The sections were then heated in boiled water and Immunosaver (Nishin EM, Tokyo, Japan) at 98°C for 45 min. Non-specific binding sites were blocked by incubating with Protein Block Serum-Free (DAKO, Carpinteria, CA, USA) for 30 min. A mouse monoclonal anti-STMN1 (OP18) antibody (Santa Cruz Biotechnology, Santa Cruz, CA, USA) and a mouse monoclonal anti-p27 antibody (Santa Cruz Biotechnology) were applied at a dilution of 1:100 for 24 h at 4°C. The primary antibody was visualized using the Histofine Simple Stain PO (M) Kit (Nichirei, Tokyo, Japan) according to the instruction manual. The chromogen 3,3¢-diaminobenzidine tetrahydrochloride was applied as a 0.02% solution containing 0.005% H_2O_2 in 50 mM ammonium acetate-citrate acid buffer (pH 6.0). The sections were lightly counterstained with Mayer's hematoxylin and mounted. Negative controls were established by omitting the primary antibody and no detectable staining was evident. We previously confirmed that esophageal carcinomas express STMN1 and p27; therefore, esophageal carcinomas were used as a positive control (Figs S1–S3).

Immunohistostaining results were evaluated as described by Altan *et al.*[22] The intensity of cytoplasmic STMN1, nuclear p27 and cytoplasmic p27 staining was scored as follows: 0, no staining; 1+, weak staining; 2+, moderate staining; and 3+, strong staining relative to the positive control (Figs S1–S3). The percentage of nuclear-stained cells was calculated by examining at least 1000 cancer cells in five representative areas. Cytoplasmic STMN1, nuclear p27 and cytoplasmic p27 were scored as follows: 0, no staining; 1+, 1–10%; 2+, 11–50%; and 3+, 51–100%. The score was defined as the percentage score multiplied by the intensity score according to the criteria presented in Table S1 (0, 1+, 2+, 3+, 4+, 6+ and 9+). The optimal cut-off point was defined as follows: grades 0, 1, 2, 3 and 4 were considered low expression, while grades 6 and 9 were designated as high expression. All samples were evaluated by two observers (AW, TY). The Ki-67 labeling index was used to calculate the percentage of cells with high nuclear expression cells in approximately 1000 cells per sample.[23]

Cell culture. The human EHCC cell line HuCCT-1 was used in the present study. All cells were obtained from RIKEN BRC through the National Bio-Resource Project of MEXT, Tokyo, Japan. The cells were cultured in RPMI 1640 medium (Wako, Osaka, Japan) supplemented with 10% FBS and 1% penicillin–streptomycin (Invitrogen, Carlsbad, CA, USA).

siRNA transfection. STMN1-specific siRNA (Silencer Pre-designed siRNA) was purchased from Bonac Corporation (Fukuoka, Japan). HuCCT-1 cells were seeded in six-well, flat-bottom microtiter plates at a density of 1×10^5 cells per well in a volume of 2 mL and incubated in a humidified atmosphere (37°C and 5% CO_2). After incubation, 500 μL of Opti-MEM I Reduced Serum Medium (Invitrogen), 5 μL Lipofectamine RNAi MAX (Invitrogen) and 5 μL STMN1-specific siRNA (50 nM final concentration in each well) were mixed and incubated for 20 min to form chelate bonds. The siRNA reagents were then added to the cells. The experiments were performed after 24–96 h of incubation.

Proximity ligation assay (PLA). HuCCT1 cells were seeded and incubated on Chamber Slides (Lab-Tek II, Thermo Scientific, Waltham, MA, USA) for 24 h. The cells were fixed with 4% paraformaldehyde for 30 min and 100% methanol for 10 min. The slides were then blocked in 4% bovine serum albumin (Millipore, Billerica, MA, USA) for 30 min and incubated for 48 h at 4°C with the appropriate combinations of mouse, rabbit and goat antibodies diluted 1:100 (STMN1 rabbit antibody; Cell Signaling Technology, Danvers, MA, USA; and p27 mouse antibody; Santa Cruz Biotechnology) in antibody dilution solution (Olink Bioscience, Uppsala, Sweden). After washing, the slides were incubated with Duolink PLA Rabbit MINUS and PLA Mouse PLUS proximity probes (Olink Bioscience) and a proximity ligation was performed using the Duolink Detection Reagent Kit (Olink Bioscience) according to the manufacturer's protocol. Nuclei were stained with Duolink In Situ Mounting Medium with DAPI (Olink Bioscience). Images were acquired with an All-in-one Fluorescence Microscope (Keyence Corporation, Osaka, Japan).

Protein extraction and western blot analysis. Transfected cells were incubated for 96 h. Total protein was extracted using the PRO-PREP Protein Extraction Solution Kit (iNtRON Biotechnology, Sungnam, Kyungki-Do, Korea) and nuclear protein was extracted with the NE-PER Nuclear and Cytoplasmic Extraction Kit (Thermo Scientific, Kanagawa, Japan). The proteins were separated on 4–12% Bis-Tris Mini Gels (Life Technologies Corporation, Carlsbad, CA, USA) and transferred to membranes using an iBlot Dry Blotting System (Life Technologies Corporation). The membranes were incubated overnight at 4°C with mouse monoclonal antibodies against STMN1 (1:1000; Santa Cruz Biotechnology), p27 (1:1000; Santa Cruz Biotechnology), β-actin (1:1000; Sigma, St Louis, MO, USA) and Histone H1 (1:1000; Santa Cruz Biotechnology). The membranes were then treated with horseradish peroxidase-conjugated anti-mouse secondary antibodies and the proteins were detected with the ECL Prime Western Blotting Detection System (GE Healthcare, Tokyo, Japan).

Proliferation assay. Cell proliferation was measured with the Cell Counting Kit-8 (Dojindo Laboratories, Kumamoto, Japan). At 48 h after transfection, the HuCCT1 cells were plated (approximately 5000 cells per well) in 96-well plates in 100 μL of medium containing 10% FBS. Evaluations were performed at the following time points: 0, 24, 48, 72 and 96 h. To determine cell viability, 10 μL of cell counting solution was added to each well and incubated at 37°C for 2 h. Next, the absorbance of each well was detected at 450 nm using a xMark Microplate Absorbance Spectrophotometer (Bio Rad, Hercules, CA, USA).

Paclitaxel assay. A water-soluble tetrazolium (WST)-8 test and the Cell Counting Kit-8 (Dojindo Laboratories) were used to evaluate paclitaxel sensitivity. At 48 h after transfection, HuCCT1 cells were seeded (10 000 cells/well) into 96-well

plates in 100 μL medium containing 10% FBS prior to drug exposure. After 24 h pre-incubation the cells were treated with various concentrations of paclitaxel for 48 h. Then, 10 μL WST-8 reagent was added and the cells were incubated for an additional 2 h at 37°C. Viability was determined using colorimetry by absorbance at 450 nm (xMark Microplate Absorbance Spectrophotometer).

Statistical analysis. Data for the continuous variables are expressed as the mean ± SEM. Significance was determined using Student's *t*-tests and ANOVA. Statistical analysis of the immunohistochemical staining data was performed using the chi-squared test. Survival curves were calculated using the Kaplan–Meier method and analyzed with the log-rank test. Prognostic factors were examined by univariate and multivariate analyses using a Cox proportional hazards model. All differences were deemed significant at $P < 0.05$ and all statistical analyses were performed with JMP software, version 5.01 (SAS Institute Inc., Cary, NC, USA).

Results

Immunohistochemical staining of STMN1 and p27 in EHCC tissues. STMN1 expression was evaluated using immunohistochemistry in 80 EHCC samples. Thirty-three samples (41.2%) were negative for STMN1 expression (Fig. 1a) and 47 samples (58.8%) were positive for cytoplasmic STMN1 expression (Fig. 1b). Nuclear p27 expression was also evaluated in these samples. Twenty-five (31.2%) samples were positive for p27 expression (Fig. 1c) and 55 samples (68.8%) were negative (Fig. 1d). High STMN1 expression was associated with low p27 nuclear expression ($P = 0.0011$; Table 1). Cytoplasmic p27 expression was evaluated in the same EHCC samples; 43 (54.4%) samples demonstrated high cytoplasmic staining for p27 expression (Fig. 1d), whereas 36 (45.6%) samples exhibited low p27 expression (Fig. 1c). High STMN1 expression was associated with high p27 cytoplasmic expression ($P = 0.0063$; Table 1).

STMN1 expression correlates with venous invasion and Ki-67 labeling index in EHCC tissues. The correlations between STMN1 expression and clinicopathological findings are shown in Table 1. We considered the following factors: patient age, patient gender, tumor stage, lymph node metastasis, lymphatic invasion, venous invasion, nerve invasion, infiltrating type and TNM stage (UICC 7th).[21] The results showed a correlation between high STMN1 expression and venous invasion ($P = 0.0021$). We also examined the association between STMN1 expression and the Ki-67 labeling index to evaluate proliferation. High-STMN1-expressing patients had a significantly higher Ki-67 labeling index in comparison to low-STMN1-expressing patients ($P < 0.0001$).

Prognostic significance of STMN1 expression in EHCC. The prognostic significance of STMN1 expression on postoperative recurrence-free survival (RFS) and cancer-specific survival (CSS) is shown in Figure 2. The STMN1-positive group had significantly poorer prognoses than the STMN1-negative group, regarding both RFS ($P = 0.0222$) and CSS ($P = 0.0061$). For CSS, STMN1 expression was prognostic for poor survival in the univariate analysis (Table 2; $P = 0.0044$). Multivariate analysis also showed STMN1 expression is prognostic for poor survival (Table 2; $P = 0.0165$). Interestingly, other existing clinicopathological factors were not significantly and independently associated with shorter CSS, whereas STMN1 expression in EHCC remained more significant than the presence of lymph node metastasis (Table 2; hazard ratio [HR], 1.696; 95% confidence interval [CI], 1.10–2.76).

STMN1 and p27 cross-interact in cultured EHCC cells. To examine the protein complexes of STMN1 and p27 in HuCCT1 cells, we performed PLA, which revealed the complexes as red spots in the cytoplasm (Fig. 3a). Thus, STMN1 interacts with p27 in the cytoplasm, but not in the nucleus, of EHCC cells.

siRNA-mediated STMN1 suppression and p27 expression in HuCCT-1 cells. Two siRNA complexes were used to knock down STMN1 expression in HuCCT-1 cells. Suppression of STMN1 by siRNA1 and siRNA2 was demonstrated using western blotting 96 h after transfection (Fig. 3b). Next, we examined the effect of STMN1 knockdown on p27 expression. STMN1 depletion induced total p27 protein expression and

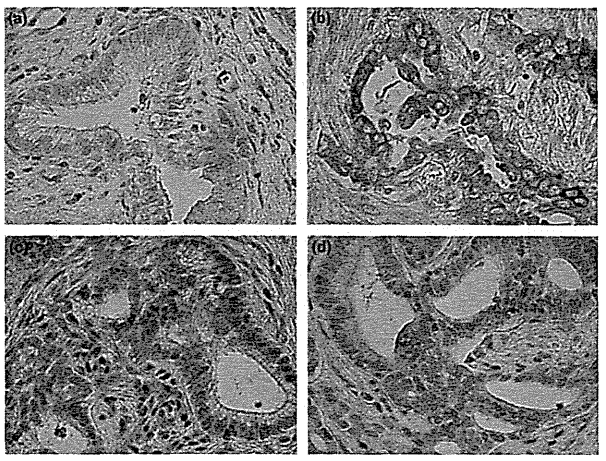

Fig. 1. Immunohistochemical staining of stathmin1 (STMN1) and p27 in primary extrahepatic cholangiocarcinoma (EHCC) samples. (a) Low STMN1 expression in a primary EHCC specimen (original magnification, ×400). (b) High STMN1 expression in a primary EHCC specimen (original magnification, ×400). (c) High nuclear p27 expression and low cytoplasmic p27 expression in a primary EHCC specimen (original magnification, ×400). (d) Low nuclear p27 expression and high cytoplasmic p27 expression in a primary EHCC specimen (original magnification, ×400). Figures a, c and b, d show images from the same cases.

Table 1. Clinicopathological characteristics of extrahepatic cholangiocarcinoma patients according to stathmin expression

Factor	STMN1 low expression (n = 33)	STMN1 high expression (n = 47)	P-value
Age (years)			
≤65	13	18	0.9211
>65	20	29	
Sex			
Male	23	35	0.6389
Female	10	12	
Differentiation			
Well	9	9	0.2563
Moderate	15	26	
Poor	8	14	
Tumor stage			
T1–2	20	19	0.0745
T3–4	13	28	
Lymph node metastasis			
–	19	27	0.9908
+	14	20	
Lymphatic invasion			
–	7	4	0.1070
+	26	43	
Venous invasion			
–	12	4	0.002*
+	21	43	
Distant metastasis			
–	32	45	0.7740
+	1	2	
Infiltration			
α	0	2	0.1179
β	17	31	
γ	15	14	
TNM stage (UICC)			
0, I	11	11	0.3297
II, III, IV	22	36	
Nuclear p27			
High expression	17	8	0.001*
Low expression	16	39	
Cytoplasmic p27			
High expression	12	31	0.006*
Low expression	21	15	
Ki-67 labeling index (mean ± SD)	9.28 ± 13.5	62.1 ± 31.9	<0.0001*

*P < 0.05. STMN1, stathmin1; TNM, tumor–node–metastasis; UICC, Union for International Cancer Control.

also had a tendency to increase nuclear p27 expression (Fig. 3b).

Suppression of STMN1 reduces proliferation and sensitizes EHCC cells to paclitaxel. We assessed the relationship between EHCC proliferation and STMN1 expression. WST assays revealed that the proliferation of STMN1-knockdown cells was significantly lower than in the parent and negative-control cells (P < 0.01; Fig. 3c). STMN1-knockdown cells were also significantly more sensitive to paclitaxel than the control cells (P < 0.01; Fig. 3d).

Immunohistochemical staining of STMN1 and p27 in EHCC tissues. STMN1 expression was evaluated using immunohistochemistry in 80 EHCC samples. Overall, 33 (41.2%) EHCC samples were negative for STMN1 expression (Fig. 1a), whereas 47 (58.8%) samples exhibited positive cytoplasmic staining for STMN1 expression (Fig. 1b). Nuclear p27 expression was also evaluated in the 80 EHCC samples. Twenty-five (31.2%) samples demonstrated positive nucleic staining for p27 expression (Fig. 1c), whereas 55 (68.8%) samples were negative for p27 expression (Fig. 1d). Moreover, the samples exhibiting high STMN1 expression were associated with low p27 nuclear expression (P = 0.0011; Table 1). In addition, p27 expression was also evaluated on each EHCC samples, 43 (54.4%) samples demonstrated high cytoplasmic staining for p27 expression (Fig. 1d), whereas 36 (45.6%) samples were low staining for p27 expression (Fig. 1c). The samples exhibiting high STMN1 expression were also associated with high p27 cytoplasmic expression (P = 0.0063; Table 1).

STMN1 expression correlates with venous invasion and Ki-67 labeling index in EHCC tissues. The correlations between STMN1 expression and clinicopathological findings are displayed in Table 1. Regarding the clinicopathological findings, we considered the following factors: patient age, patient gender, tumor stage, lymph node metastasis, lymphatic invasion, venous invasion, nerve invasion, infiltrating type and TNM stage (UICC 7th). The results revealed that STMN1-high expression was correlated with venous invasion (P = 0.0021). In addition, we examined the association between STMN1 expression and the Ki-67 labeling index to evaluate proliferation ability. The STMN1-high-expression patients had a significantly higher Ki-67 labeling index than the low-expression patients (P < 0.0001).

Prognostic significance of STMN1 expression in EHCC. The prognostic significance of STMN1 expression on postoperative RFS and CSS rates are displayed in Figure 2. The STMN1-positive group had significantly poorer prognoses than the STMN1-negative group, regarding both RFS (P = 0.0222) and CSS (P = 0.0061). For CSS, STMN1 expression was a prognostic factor for poor survival in the univariate analysis (Table 2; P = 0.0044). In the multivariate analysis, STMN1 expression was also a prognostic factor for poor survival (Table 2; P = 0.0165). Interestingly, other existing clinicopathological factors were not significantly and independently associated with shorter CSS, whereas the detection of STMN1 expression in EHCC remained prognostically more significant than the presence of lymph node metastasis with regard to CSS (Table 2; HR, 1.696; 95% CI, 1.10–2.76).

STMN1 and p27 cross-interactinn EHCC cells *in vitro*. To examine the protein complexes formed between STMN1 and p27 in HuCCT1 cells, we performed PLA. As a result, the formations of STMN1 and p27 complexes were detected in the cytoplasm as red spots (Fig. 3a). This result demonstrates that STMN1 interacts with p27 in the cytoplasm, but not in the nucleus, of EHCC cells.

Effect of siRNA-mediated STMN1 suppression on p27 expression in HuCCT-1 cells. Two siRNA complexes were used to knockdown *STMN1* expression in the HuCCT-1 cells. The suppression of STMN1 by siRNA1 and siRNA2 was demonstrated using western blotting 96 h after transfection (Fig. 3b). Next, we examined the effect of *STMN1* knockdown on p27 expression. The depletion of STMN1 increased p27 expression on total protein and also had a tendency to increase nuclear p27 expression (Fig. 3b).

Suppression of STMN1 reduces proliferation and sensitizes EHCC cells to paclitaxel. We assessed the relationship between the proliferative ability of EHCC cells and STMN1 expression. The cellular proliferation ability was evaluated using the WST assay, which revealed that the proliferation of *STMN1*-knockdown cells significantly diminished compared with the

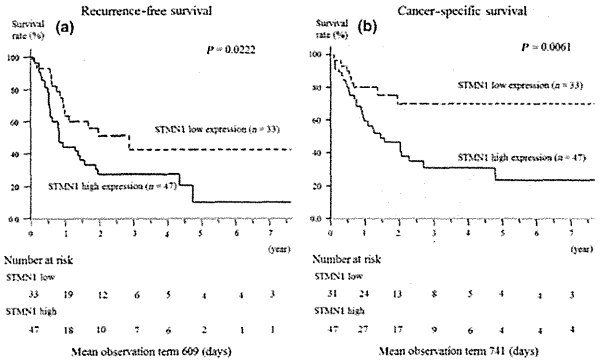

Fig. 2. Relationship between postoperative survival and stathmin1 (STMN1) expression. Kaplan–Meier curves of the low-STMN1-expression and high-STMN1-expression groups are shown. (a) High STMN1 expression indicated a poor prognosis for recurrence-free survival ($P = 0.0222$). (b) High STMN1 expression also indicated a poor prognosis for cancer-specific survival ($P = 0.0061$).

Table 2. Univariate and multivariate analysis of prognostic factors using the Cox proportional hazards model

Factor	Univariate analysis			Multivariate analysis		
	RR	95% CI	*P*-value	RR	95% CI	*P*-value
Age (≤65/>66)	0.994	0.70–1.38	0.9720	–	–	–
Sex (M/F)	0.753	0.49–1.09	0.1392	–	–	–
Tumor stage (T1–2/3–4)	2.314	1.18–4.71	0.0131*	2.031	0.97–4.39	0.0577
Lymph node metastasis (−/+)	1.742	1.23–2.50	0.0013*	1.48	1.02–2.20	0.0379*
Lymphatic invasion (−/+)	1.631	0.97–3.33	0.0649	–	–	–
Venous invasion (−/+)	1.619	1.02–2.97	0.0410*	1.039	0.59–1.99	0.898
Distant metastasis (−/+)	1.803	0.29–5.99	0.4582	–	–	–
Adjuvant therapy (−/+)	0.467	0.25–0.90	0.0242*	0.346	0.17–0.70	0.0035*
Nuclear p27 expression (−/+)	0.596	0.36–0.89	0.0011*	0.811	0.47–1.30	0.401
STMN1 expression (−/+)	1.688	1.16–2.58	0.0044*	1.696	1.10–2.76	0.0165*

*$P < 0.05$. CI, confidence interval; RR, relative risk; STMN1, stathmin1.

parent and negative-control cells ($P < 0.01$; Fig. 3c). Moreover, *STMN1*-knockdown cells exhibited significantly higher sensitivity to paclitaxel than the control cells ($P < 0.01$; Fig. 3d).

Discussion

In the present study, we demonstrated that high STMN1 expression is associated with poor prognosis in primary EHCC samples. Moreover, high STMN1 expression is related to low nuclear p27 expression and high cytoplasmic p27 expression. In the *in vitro STMN1* knockdown analysis, proliferative ability was reduced and paclitaxel sensitivity was increased in transfected cells compared with the control cells. In addition, *STMN1* knockdown increased p27 expression.

In the immunohistochemical analysis, high STMN1 expression correlated to poor RFS and CSS prognosis. Moreover, based on the multivariate analysis of CSS, high STMN1 expression translated into an independent prognostic factor. Some reports have also revealed that high STMN1 expression is related to poor prognosis in the following cancers: oral squamous cell carcinoma;[13] diffuse type gastric cancer;[9] colon cancer;[14] hepatocellular cancer;[12] and urothelial carcinoma.[17] The results of the present study are in agreement with these previous reports. Therefore, STMN1 is expected to serve as a prognostic-predictive marker of EHCC.

In the present study, high STMN1 expression was associated with venous invasion in EHCC. Jeon *et al.*[9] reported this association in diffuse type gastric carcinoma and showed that *in vitro* STMN1 suppression inhibited migration and invasion in gastric cancer cells. Baldassare *et al.*[18] reported that STMN1 promotes invasion in sarcoma and regulates microtubule stability following adhesion to the extracellular matrix. STMN1 also regulated invasion in hepatocellular carcinoma.[12] Our results were consistent with these previous reports and indicate that STMN1 is associated with invasion in EHCC.

Previous studies have examined the relationship between STMN1 and p27.[24,25] Baldassarre *et al.*[18] reported that STMN1 bound to p27 in the cytoplasm of sarcoma cells and that high-STMN1-expressing and low-p27-expressing cells demonstrate increased proliferation and invasion ability. However, the authors did not describe in detail whether cytoplasmic p27 regulates STMN1 function or whether cytoplasmic STMN1 inhibits the import of p27 into the nucleus. In our immunohistochemical analysis of EHCC, high-STMN1-expressing samples exhibited a significant tendency for low nuclear p27 expression and high cytoplasmic p27 expression. Using a PLA assay, STMN1 was

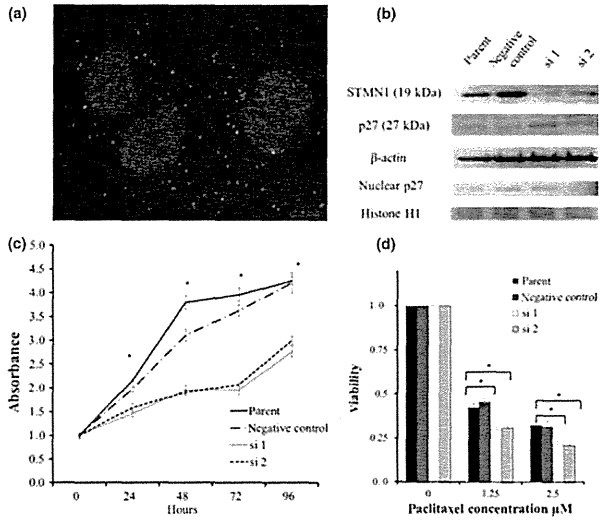

Fig. 3. (a) Stathmin1 (STMN1) bound to p27 in the cytoplasm of HuCCT1 cells. Primary STMN1 rabbit and p27 mouse antibodies bound to STMN1 and p27 complexes were combined with secondary proximity ligation assay probes. The interaction events are visible as red dots (nuclear staining with DAPI). (b) siRNA-mediated STMN1 suppression. STMN1 protein levels were measured using western blotting after transfection with STMN1 siRNA. p27 expression in STMN1 siRNA-transfected and untreated HuCCT-1 cells was assessed using western blotting of total and nuclear protein. β-Actin was used as a loading control for total protein and Histone H1 was used as a loading control for nuclear protein. (c) HuCCT-1 cells were transfected with STMN1 siRNA and WST-8 proliferative assays were performed and compared with untransfected cells. (d) Paclitaxel sensitivity was determined using a WST-8 assay. STMN1 siRNA transfection significantly increased paclitaxel sensitivity compared with untransfected cells. Each time point represents the mean ± SD of triplicate determinations in two independent experiments. $^*P < 0.05$.

shown to interact with p27 directly in the cytoplasm of HuCCT1 cells *in vitro*. Moreover, siRNA-mediated *STMN1* knockdown triggered increased p27 expression and the proliferative ability of STMN1-suppressed cells significantly diminished. Interestingly, p27-degradation promotion has been reported in the cytoplasm but not in the nucleus during the G0–G1 transition. From these results it is suggested that STMN1 interacts with p27 in the cytoplasm, inhibits the function of nuclear p27 via the degradation of cytoplasmic p27 and leads to the progression of cancer. S phase kinase-associated protein 2 (SKP2) promotes p27 degradation via the ubiquitin–proteasome system[26] and p27 upregulation facilitated by a SKP2 inhibitor significantly suppresses the cell cycle and results in lower proliferation potency.[27] Therefore, p27 regulation by STMN1 targeting might provide a promising therapeutic tool for several cancers including EHCC.

Some studies have examined the relationship between STMN1 expression and taxane anticancer drugs. STMN1 overexpression levels are associated with paclitaxel sensitivity in ovarian cancer and breast cancer cells.[6,28] Iancu *et al.*[29] reported that taxol and anti-STMN1 therapy produced a synergistic anticancer effect on a leukemic cell line. Moreover, Alli *et al.*[7] also reported that STMN1 overexpression increases the rate of cell death, decreases microtubule polymerization, which markedly decreases taxane binding, and prevents cells from entering mitosis. In the present study, *STMN1* knockdown increased paclitaxel sensitivity, which is consistent with previous reports. Although few anti-microtubule cancer drugs have produced a positive effect on EHCC in current clinical practice, the combination of taxane and anti-STMN1 drugs may provide a prospective therapy against various cancers in the future.

In conclusion, STMN1 expression contributed to a shorter duration of RFS and reduced CSS in patients with EHCC. Therefore, the evaluation of STMN1 expression in EHCC might be a useful predictor of recurrence and poor prognosis. Moreover, high STMN1 expression was associated with low p27 expression in clinical EHCC samples and STMN1 suppression regulated proliferation and paclitaxel sensitivity in an EHCC cell line. Our results suggest that STMN1 in EHCC may be a promising molecular target for controlling cancer progression and taxane resistance via p27 regulation.

Acknowledgments

The authors thank Ms Yukie Saito, Ms Tomoko Yano, Ms Tomoko Ubukata, Ms Yuka Matsui, Ms Ayaka Ishida and Ayaka Ishikubo for their excellent assistance.

Disclosure Statement

The authors have no conflicts of interest.

References

1 Vasilieva LE, Papadhimitriou SI, Dourakis SP. Modern diagnostic approaches to cholangiocarcinoma. *Hepatobiliary Pancreat Dis Int* 2012; **11**: 349–59.
2 Skipworth JR, Olde Damink SW, Imber C, Bridgewater J, Pereira SP, Malago M. Review article: surgical, neo-adjuvant and adjuvant management strategies in biliary tract cancer. *Aliment Pharmacol Ther* 2011; **34**: 1063–78.
3 Pichlmayr R, Weimann A, Klempnauer J *et al.* Surgical treatment in proximal bile duct cancer. A single-center experience. *Ann Surg* 1996; **224**: 628–38.
4 Klempnauer J, Ridder GJ, Werner M, Weimann A, Pichlmayr R. What constitutes long-term survival after surgery for hilar cholangiocarcinoma? *Cancer* 1997; **79**: 26–34.
5 Alli E, Yang JM, Hait WN. Silencing of stathmin induces tumor-suppressor function in breast cancer cell lines harboring mutant p53. *Oncogene* 2007; **26**: 1003–12.

6 Alli E, Yang JM, Ford JM, Hait WN. Reversal of stathmin-mediated resistance to paclitaxel and vinblastine in human breast carcinoma cells. *Mol Pharmacol* 2007; **71**: 1233–40.
7 Alli E, Bash-Babula J, Yang JM, Hait WN. Effect of stathmin on the sensitivity to antimicrotubule drugs in human breast cancer. *Cancer Res* 2002; **62**: 6864–9.
8 Ghosh R, Gu G, Tillman E *et al.* Increased expression and differential phosphorylation of stathmin may promote prostate cancer progression. *Prostate* 2007; **67**: 1038–52.
9 Jeon TY, Han ME, Lee YW *et al.* Overexpression of stathmin1 in the diffuse type of gastric cancer and its roles in proliferation and migration of gastric cancer cells. *Br J Cancer* 2010; **102**: 710–8.
10 Kang W, Tong JH, Chan AW *et al.* Stathmin1 plays oncogenic role and is a target of microRNA-223 in gastric cancer. *PLoS ONE* 2012; **7**: e33919.
11 Singer S, Ehemann V, Brauckhoff A *et al.* Protumorigenic overexpression of stathmin/Op18 by gain-of-function mutation in p53 in human hepatocarcinogenesis. *Hepatology* 2007; **46**: 759–68.
12 Hsieh SY, Huang SF, Yu MC *et al.* Stathmin1 overexpression associated with polyploidy, tumor-cell invasion, early recurrence, and poor prognosis in human hepatoma. *Mol Carcinog* 2010; **49**: 476–87.
13 Kouzu Y, Uzawa K, Koike H *et al.* Overexpression of stathmin in oral squamous-cell carcinoma: correlation with tumour progression and poor prognosis. *Br J Cancer* 2006; **94**: 717–23.
14 Zheng P, Liu YX, Chen L *et al.* Stathmin, a new target of PRL-3 identified by proteomic methods, plays a key role in progression and metastasis of colorectal cancer. *J Proteome Res* 2010; **9**: 4897–905.
15 Ogino S, Nosho K, Baba Y *et al.* A cohort study of STMN1 expression in colorectal cancer: body mass index and prognosis. *Am J Gastroenterol* 2009; **104**: 2047–56.
16 Kim JY, Harvard C, You L *et al.* Stathmin is overexpressed in malignant mesothelioma. *Anticancer Res* 2007; **27**: 39–44.
17 Lin WC, Chen SC, Hu FC *et al.* Expression of stathmin in localized upper urinary tract urothelial carcinoma: correlations with prognosis. *Urology* 2009; **74**: 1264–9.
18 Baldassarre G, Belletti B, Nicoloso MS *et al.* p27(Kip1)-stathmin interaction influences sarcoma cell migration and invasion. *Cancer Cell* 2005; **7**: 51–63.
19 Nakayama K, Ishida N, Shirane M *et al.* Mice lacking p27(Kip1) display increased body size, multiple organ hyperplasia, retinal dysplasia, and pituitary tumors. *Cell* 1996; **85**: 707–20.
20 Denicourt C, Dowdy SF. Cip/Kip proteins: more than just CDKs inhibitors. *Genes Dev* 2004; **18**: 851–5.
21 Sobin LH, Gospodarowicz MK, Wittekind C, eds. *TMN Classification of Malignant Tumors*, 7th edn. Washington, DC: Wiley-Blackwell, 2009.
22 Altan B, Yokobori T, Mochiki E *et al.* Nuclear karyopherin-alpha2 expression in primary lesions and metastatic lymph nodes was associated with poor prognosis and progression in gastric cancer. *Carcinogenesis* 2013; **34**: 2314–21.
23 Suzuki S, Miyazaki T, Tanaka N *et al.* Prognostic significance of CD151 expression in esophageal squamous cell carcinoma with aggressive cell proliferation and invasiveness. *Ann Surg Oncol* 2011; **18**: 888–93.
24 Iancu-Rubin C, Atweh GF. p27(Kip1) and stathmin share the stage for the first time. *Trends Cell Biol* 2005; **15**: 346–8.
25 Karst AM, Levanon K, Duraisamy S *et al.* Stathmin 1, a marker of PI3K pathway activation and regulator of microtubule dynamics, is expressed in early pelvic serous carcinomas. *Gynecol Oncol* 2011; **123**: 5–12.
26 Hara T, Kamura T, Nakayama K, Oshikawa K, Hatakeyama S. Degradation of p27(Kip1) at the G(0)–G(1) transition mediated by a Skp2-independent ubiquitination pathway. *J Biol Chem* 2001; **276**: 48937–43.
27 Wu L, Grigoryan AV, Li Y, Hao B, Pagano M, Cardozo TJ. Specific small molecule inhibitors of Skp2-mediated p27 degradation. *Chem Biol* 2012; **19**: 1515–24.
28 Balachandran R, Welsh MJ, Day BW. Altered levels and regulation of stathmin in paclitaxel-resistant ovarian cancer cells. *Oncogene* 2003; **22**: 8924–30.
29 Iancu C, Mistry SJ, Arkin S, Atweh GF. Taxol and anti-stathmin therapy: a synergistic combination that targets the mitotic spindle. *Cancer Res* 2000; **60**: 3537–41.

Supporting Information

Additional supporting information may be found in the online version of this article:

Fig. S1. Immunohistochemical staining of stathmin1 (STMN1) in primary esophageal cancer served as a positive control.

Fig. S2. Immunohistochemical staining of nuclear p27 in primary esophageal cancer served as a positive control.

Fig. S3. Immunohistochemical staining of cytoplasmic p27 in primary esophageal cancer served as a positive control.

Table S1. Criteria of Immunohisochemistry evaluation.

J Neurosurg 120:1298–1308, 2014

Enhanced expression of proapoptotic and autophagic proteins involved in the cell death of glioblastoma induced by synthetic glycans

Laboratory investigation

Ahmad Faried, M.D., Ph.D.,[1] Muhammad Zafrullah Arifin, M.D., Ph.D.,[1] Shogo Ishiuchi, M.D., Ph.D.,[2] Hiroyuki Kuwano, M.D., Ph.D.,[3] and Shin Yazawa, Ph.D.[3,4]

[1]Department of Neurosurgery, Faculty of Medicine, Universitas Padjadjaran–Dr. Hasan Sadikin Hospital, Bandung, Indonesia; [2]Department of Neurosurgery, Faculty of Clinical Medicine, the University of Ryukyus, Nakagami-gun, Okinawa; [3]Department of General Surgical Science, Faculty of Medicine, Gunma University, Maebashi; and [4]Tokushima Research Institute, Otsuka Pharmaceutical Co. Ltd., Tokushima, Japan

Object. Glioblastoma is the most aggressive malignant brain tumor, and overall patient survival has not been prolonged even by conventional therapies. Previously, the authors found that chemically synthesized glycans could be anticancer agents against growth of a series of cancer cells. In this study, the authors examined the effects of glycans on the growth of glioblastoma cells both *in vitro* and *in vivo*.

Methods. The authors investigated not only the occurrence of changes in the cell signaling molecules and expression levels of various proteins related to cell death, but also a mouse model involving the injection of glioblastoma cells following the administration of synthetic glycans.

Results. Synthetic glycans inhibited the growth of glioblastoma cells, induced the apoptosis of the cells with cleaved poly (adenosine diphosphate-ribose) polymerase (PARP) expression and DNA fragmentation, and also caused autophagy, as shown by the detection of autophagosome proteins and monodansylcadaverine staining. Furthermore, tumor growth in the in vivo mouse model was significantly inhibited. A dramatic induction of programmed cell death was found in glioblastoma cells after treatment with synthetic glycans.

Conclusions. These results suggest that synthetic glycans could be a promising novel anticancer agent for performing chemotherapy against glioblastoma.
(http://thejns.org/doi/abs/10.3171/2014.1.JNS131534)

Key Words • **synthetic glycan** • **glioblastoma** • **apoptosis** • **autophagy** • **oncology**

Glioblastoma is the most aggressive and lethal malignancy of the CNS, and patients with glioblastoma have an average life expectancy of 1 year after the standard treatment of surgery followed by radiation therapy.[26,45] Recently, clinical studies have shown that chemotherapy in addition to radiation therapy could increase patient survival up to 2 years.[45] The continuing problems caused by glioblastoma and the failure of conventional therapy for this advanced invasive brain tumor indicate that novel strategies and anticancer drugs are critically needed to improve the prognosis.

Glioblastoma cells are naturally resistant to cell death,[16,26] which has been considered to be attributable to the activation of phosphatidylinositol 3-kinase (PI3K) by growth factors and the subsequent hyperactivation of its downstream targets, the serine/threonine kinases protein kinase B (Akt) and mammalian target of rapamycin (mTOR). These targets are known to release a variety of

Abbreviations used in this paper: Akt = protein kinase B; AMPA = α-amino-3-hydroxy-5-methyl-4-isoxazolepropionic acid; CPI = cell proliferation inhibition; HP-β-CD = hydroxypropyl-β-cyclodextrin; GalβChol = D-galactose β cholestanol; GChol = GlcNAcβChol; GGChol = GlcNAcβ1,3 GalβChol; GlcNAcβ1,3 = *N*-acetyl-D-glucosamine β1,3; GluR1 = glutamate receptor 1; GluR4 = glutamate receptor 4; HO342 = Hoechst 33342; MDC = monodansylcadaverine; mTOR = mammalian target of rapamycin; PARP = poly (adenosine diphosphate-ribose) polymerase; PI3K = phosphatidylinositol 3-kinase; Z-VAD-FMK = benzyloxycarbonyl-Val-Ala-Asp(OMe)-fluoromethylketone.

This article contains some figures that are displayed in color online but in black-and-white in the print edition.

antiapoptotic signals, thereby promoting the proliferation of the tumor cells.[26,34,39] Growing evidence is accumulating that glioblastoma cells exploit glutamate for their proliferation and migration ability. The released glutamate may stimulate glioblastoma cell growth and migration through the autocrine and/or paracrine activation of glutamate receptors.[20,21] In addition, the expression of Rho GTPase family members has been demonstrated in a wide variety of malignancies[9,12,18,23] and in high-grade glioma as a hallmark of cell migration and as a predictor of the clinical prognosis.[47]

Programmed cell death plays an important role during tissue development and homeostasis. Aberrations in this process result in the pathology of numerous disorders, such as malignancy. Apoptosis is the most common form of programmed cell death, but recently, alternative cell death programs have received increased attention, with autophagy proposed as an important nonapoptotic cell death mechanism.[6,33]

In our previous studies, using chemically synthesized glycans consisting of sugar cholestanols with mono-, di-, and trisaccharides attached to cholestanols, we showed both strong inhibitory activity against the proliferation of a series of mouse and human cancer cells from the digestive system and antitumor effects in a mouse model of peritoneal dissemination.[8,14,15] The sugar cholestanols added to the cell culture were rapidly taken up via the lipid rafts/microdomains on the cell surface.[15] The uptake of sugar cholestanols in mitochondria increased gradually and was followed by the activation of apoptotic signals via the caspase cascade, leading to apoptotic cell death.[8,14,15] Furthermore, the examination of sugar cholestanols in a mouse model of peritoneal dissemination showed a dramatic reduction of tumor growth and a prolonged survival time of the mice.[15] The sugar cholestanols described in our previous studies, therefore, appeared to have clinical potential as novel anticancer agents. However, the cell death pathways in malignant glioma cells induced by the same compounds remain an open question. In this study, we investigated the programmed cell death induced by the sugar cholestanols in glioblastoma cells and its anticancer effect on growth in nude mice.

Methods

Cell Lines and Culture Condition

Human glioblastoma cell lines, CGNH-89 and CGNH-NM, were established as described previously.[19,20] The morphology of CGNH cells is epithelial and adherent type, and their doubling time is 24 hours. CGNH cells were established through resection from the tumor at the right frontal lobe of female patients according to the explant method by Nichols et al.[36] It has been demonstrated that the CGNH cells have glioblastoma morphological characteristics, and they grow very fast (highly cellular) and are relatively monotonous, while some are multinucleated giant cells with slight nuclear pleomorphism, marked atypical nucleus, and brisk mitotic activity.[19,20] The cells were maintained at 37°C in DMEM (Nissui) supplemented with 10% fetal bovine serum (Invitrogen) and 3% L-glutamine in a humidified atmosphere of 5% CO_2 in air. When they were confluent, the cells were exposed in 0.05% trypsin and subcultured in the same growth medium.

Compounds

N-acetyl-D-glucosamine (GlcNAc) β1,3 D-galactose (Gal) β cholestanol, or GGChol, and GlcNAc β cholestanol, or GChol, were synthesized and prepared[13,15] as an inclusion complexation with 20% of hydroxypropyl-β-cyclodextrin (HP-β-CD; BICO) and used for the experiment as previously described.[8,15]

Antibodies and Chemical Reagents

Anti-GluR1 (glutamate receptor 1) and GluR4 (glutamate receptor 4) were obtained from Chemicon. Anti–RhoA, RhoC, Beclin-1, and LC3 were obtained from Santa Cruz Biotech, Inc. Anti-pAkt at ser473, pmTOR at ser2448, p53 at ser46, Bcl-2 family, caspase family, and poly (adenosine diphosphate-ribose) polymerase (PARP) were obtained from Cell Signaling. 3-Methyladenine (3-MA; Sigma), was used as an inhibitor of autophagy. 3-MA (30 mg) was dissolved with 1 ml dH_2O to make a 200 mM stock solution and kept at room temperature. Benzyloxycarbonyl-Val-Ala-Asp(OMe)-fluoromethylketone (Z-VAD-FMK, or just Z-VAD; BD Biosciences), a general caspase inhibitor, was used to inhibit apoptosis. Z-VAD was dissolved in dimethylsulfoxide for a stock solution. And 1 mM of 3-MA and 10 μM of Z-VAD were diluted separately in DMEM to obtain the desired concentration. The autofluorescent agent monodansylcadaverine (MDC; Sigma) was introduced as a specific autophagolysosome marker to analyze the autophagic process.[32] The fluorescence of MDC has been reported to be a specific marker for autophagic vacuoles.[1] Monodansylcadaverine was dissolved in methanol (10 mg/ml) and used to observe autophagy.

Cell Proliferation Inhibition and Nuclear Fragmentation Assays

Cell proliferation inhibition with each compound was conducted in the presence of serially diluted compounds as described previously.[8,15] DNA binding dyes, Hoechst 33342 (HO342), in addition to propropidium iodidedium iodide fluorescence, were used for determination of apoptosis.[17] Cells were exposed to HO342 (10 μM) and propidium iodide (10 μM), and each fluorescence intensity was examined using a fluorescence microscope with ultraviolet excitation at 340–380 nm. The apoptotic index (AI) was calculated as follows:

AI = apoptotic cell number ÷ (apoptotic cell number + necrotic cell number + viable cell number) × 100%

Protein Extraction and Western Blot Analysis

All cells were harvested at approximately 80% confluent growth. Protein concentrations of the cell lysate were determined with a bicinchoninic acid protein assay kit (Pierce) using bovine serum albumin as a standard. Each sample (50 μg protein/line) was run on a 5%–20% ReadyGel (Bio-Rad) and the gel was then electrotransferred to a hybond-enhanced chemiluminescence nitrocellulose

membrane (Amersham Pharmacia Biotech). Changes in expression levels of corresponding (apoptosis and autophagy) proteins after treatment with sugar cholestanol were analyzed by Western blotting; β-actin was used as a loading control. Bands on the membrane were detected using an enhanced chemiluminescence detection system, and horizontal scanning densitometry was performed using Photoshop software (version 3.0, Adobe), and analyzed by Quantity One software (BioRad).

Analysis of Autophagy

The analysis of autophagy was performed with the aid of MDC and counted as previously described.[32] Autophagic vacuoles were labeled with MDC, and the fluorescent images were obtained with an epifluorescence microscope (BX-50, Olympus). The quantification of intracellular MDC accumulation was measured by fluorometry. Cells (2×10^4) were incubated with 0.05 mM MDC in phosphate-buffered saline at 37°C for 10 minutes and collected in 10 mM Tris-HCl, pH 8.0, containing 0.1% Triton X-100. Fluorescence was measured at a 380-nm excitation wavelength with a 530-nm emission filter, using an MTP-600 microplate reader (Corona Electric). Monodansylcadaverine expression was measured using a relative unit to show the ratio of the amount on intensity from fluorescence imaging.

Antitumor Effect of Sugar Cholestanols on Nude Mice Injected With CGNH-89 Cells

The effect of sugar cholestanols on CGNH-89 cell growth was evaluated quantitatively in a subcutaneous tumor. Cell suspensions (2×10^7 cells/200 μl) were injected subcutaneously in the flanks of 5- to 6-week-old nude mice (Clea Laboratories). One hundred microliters of 2 μmol of GChol dissolved in HP-β-CD was administered intratumoraly 3 times (at 14, 15, and 16 days) after tumor inoculation with a 27-gauge needle. The same treatment of HP-β-CD without GChol was conducted as control. Tumor volume was calculated as follows: (length × width^2)/2.

At the end of each experiment, tumor tissues were subjected to histological analysis. Five mice were used for each group, and the experiment was approved by the Animal Care and Experimentation Committee of Gunma University. Experiments using patient tissues from glioblastoma cells were approved by the Ethical Committee of Gunma University.

Statistical Analysis

Statistical analysis was performed using StatView software (version 5.0, SAS Institute). Differences were considered significant when $p < 0.05$.

Results

Cell Proliferation Inhibition of Glioblastoma Cells by Sugar Cholestanols

The effects of sugar cholestanols on the viability of glioblastoma cells were evaluated at various concentrations. Sugar cholestanols such as GGChol and GChol showed considerable inhibiting activities against the proliferation of glioblastoma cells in a dose-dependent manner (Fig. 1). However, βChol itself, without the sugar moiety, showed very low activity only at a high concentration in CGNH cells (data not shown). The minimum concentrations of sugar cholestanols producing 50% cell proliferation inhibition (CPI_{50}) were determined in the glioblastoma cells, and no clear differences were observed (Table 1). The sugar cholestanols clearly induced cell death in glioblastoma cells.

Nuclear Fragmentation

Nuclear fragmentation was clearly observed in CGNH cells treated with GGChol but not in the control cells (Fig. 2 left). Staining of the glioblastoma cells (CGNH-89 and CGNH-NM) with HO342 and propidium iodide indicated that GGChol induced nuclear fragmentation (a hallmark of apoptosis) in approximately 17% and 23% of the total cells, respectively, and were counted as apoptotic (Fig. 2 right).

Western Blot Analysis of Caspase Cascade and PARP Activation

Caspase signaling pathways consisting of a death receptor–dependent extrinsic pathway and death receptor–independent intrinsic pathway were examined in the glioblastoma cells treated with GGChol. The expression levels of active caspase-8 for the extrinsic pathway, caspase-9 for the intrinsic pathway, and caspase-3 were found to increase in the CGNH-89 and CGNH-NM cells in a time-dependent manner (Fig. 3). The expression levels of PARP, one of the best biomarkers of apoptosis, were analyzed in CGNH cells during the 24 hours after the treatment with GGChol. The N-terminal fragment of PARP, possessing an 89-kDa peptide cleaved from the full-sized PARP (116 kDa), was detected as early as 2 hours in the CGNH cells after the treatment with sugar cholestanols (Fig. 3). These results suggested that GGChol induced apoptotic cell death through both extrinsic and intrinsic pathways.

Analysis of Autophagy, Apoptosis, and the Inhibition of Both

We examined the changes in autophagy activity in both CGNH-89 and CGNH-NM cells treated with GGChol. The treatment of both cell types with GGChol induced not only apoptosis but also an autophagic response (Fig. 4). In both cell types, the number of distinct dot-like structures distributed within the cytoplasm or localized in the perinuclear regions was higher than in the control (Fig. 4A and B, left). The level of MDC incorporated into the CGNH-89 and CGNH-NM cells was increased 1.4- and 1.5-fold, respectively, after being treated with GGChol compared with that in the untreated cells (Fig. 4A and B, right). The cell viability of glioblastoma cells was reduced in the presence of GGChol up to 60% but was restored after the addition of 3-MA and Z-VAD to the culture medium (Fig. 4C). Our results showed that 3-MA and Z-VAD can block autophagy and apoptosis from 17%–20% and 38%–41%, respectively. The combination of inhibitors against both autophagy and apoptosis can fully block the cell death induced by GGChol (45%–

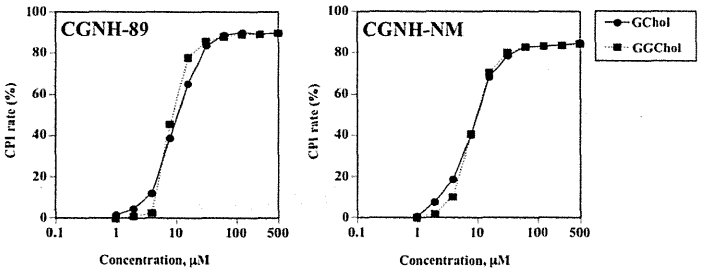

FIG. 1. Line graphs showing the effect of sugar cholestanols on the viability of glioblastoma cells. The CGNH-89 and CGNH-NM cells were treated with various concentrations of sugar cholestanols for 24 hours.

48% increase). When 3-MA and Z-VAD were added at the same time to the cell culture, the cell viability in the GGChol-treated cells was as high as that of the untreated control cells. However, no effect was observed when either agent was added individually to the cell culture (Fig. 4C).

Western Blot Analysis of the Bcl-2 Family

The expression levels of Bcl-2 family members, consisting of both proapoptosis and antiapoptosis factors, were then analyzed in the CGNH cells treated with GGChols. A slightly increased expression of Bax (proapoptosis) was detected in the CGNH-89 and CGNH-NM cells in a time-dependent manner, and a slightly decreased expression of Bcl-xL (antiapoptosis) was detected in the same cells (Fig. 5). We also evaluated the expression level of p53 (ser46), one of the initiators that activates Bax and/or downregulates Bcl-xL. Our results showed that glioblastoma cells treated with GGChol increased the expression of p53 (ser46) in a time-dependent manner (Fig. 5).

Western Blot Analysis of Autophagy

Using Western blot analysis and MDC staining, we found that GGChol increased the expression of apoptosis-related proteins and slightly increased the expression of LC3-II and Beclin-1 (Fig. 5). All these results suggest that sugar cholestanols induced both apoptosis and autophagic cell death in glioblastoma cells.

Western Blot Analysis of Survival Pathways

The expression of survival signaling proteins was evaluated in glioblastoma cells in response to sugar cholestanols. The treatment of both CGNH cell types with GGChol indicated inhibition of Akt activation and expression of both phosphorylated Akt (ser473) and phosphorylated mTOR (ser2448), the downstream targets of Akt in glioblastoma cells (Fig. 6A). The expression levels of the upstream molecules related to Akt/mTOR were also analyzed in CGNH cells treated with GGChol, and the decreased expression of both GluR1 and GluR4 was detected in CGNH cells treated with GGChol in a time-dependent manner (Fig. 6A). However, the expression levels of RhoA and RhoC in CGNH cells treated with GGChol were revealed to be suppressed in a time-dependent manner (Fig. 6B).

Antitumor Effect of Sugar Cholestanols in a Mouse Model

Nude mice were subcutaneously inoculated with CGNH-89 cells and tumors formed within 2 weeks in all

TABLE 1: Minimum amounts of each compound producing 50% cell proliferation inhibition of various cells*

	CPI_{50} (μM)	
Compounds	CGNH-89	CGNH-NM
GGChol	14.8	15.6
GChol	15.6	17.2
cholestanol	>1000	>1000

* The 3(4,5-dimethylthiazol-2-yl)2,5-diphenyltetrazolium bromide (MTT) assay was conducted after 24 hours of incubation under the presence of each compound diluted from 500 μM to 0.98 μM (in a gradual manner).

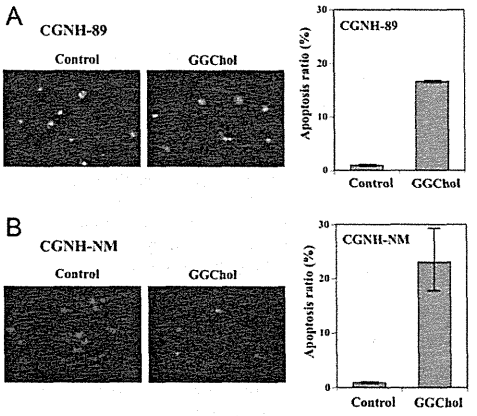

FIG. 2. **Left:** Induction of apoptotic cell death in CGNH-89 **(A)** and CGNH-NM **(B)** cells after treatment with GGChol. The cells were analyzed by the HO342 combined with propidium iodide assay. Original magnification ×200. **Right:** The apoptosis index (mean ± SEM) was calculated in each cell line. All results were from 3 independent experiments.

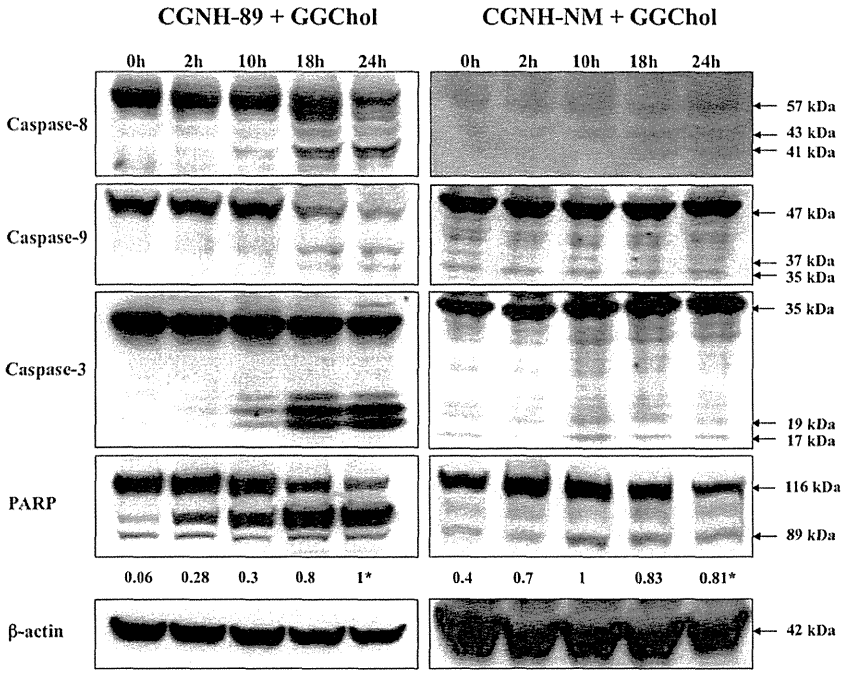

FIG. 3. Western blot analysis of glioblastoma cells treated with GGChol. The cells were treated with 30 μM of GGChol for 24 hours, and the values given below the caspase-8, -9, -3, and PARP figures indicate the calculation of the active form band (41–43 kDa, 35–37 kDa, 17–19 kDa, and 89 kDa, respectively) after normalization of its expression to that of β-actin, shown as a percentage compared with the control. *Asterisk* = significant increase for the active form of cleaved PARP (89 kDa) measured using densitometric analysis.

mice. Tumor formation was significantly suppressed ($p < 0.05$) in the mice treated with GChol in HP-β-CD intratumorally 3 times at 14, 15, and 16 days after inoculation of tumor cells. However, no significant suppression was observed in the mice treated only with HP-β-CD (Fig. 7). The histological analysis of GChol-treated mice revealed the presence of high degrees of tumor anaplasia including nuclear and cytoplasmic pleomorphism, tumor necrosis, and vascular proliferation. However, in the control mice, large numbers of mitotic cells were observed (data not shown), as hallmarks of the glioblastoma cells.

Discussion

Temozolomide is commonly used in the treatment of primary or recurrent high-grade gliomas, including anaplastic astrocytoma and glioblastoma.[2,48] To date, the prognosis of patients with malignant gliomas has been poor.[4] It is clear that tumor cells with drug-resistant ability will not respond to chemotherapy treatment. The mechanism by which temozolomide mediates cell death in malignant tumor cells has been characterized, and it was shown to induce autophagy, not apoptosis, in glioblastoma.[24] In the cancer field, autophagy is a new concept for the defense mechanisms of malignant cells,[38,40] and they are eliminated, in some cases, due to the induction of a nonapoptotic mechanism, also known as autophagic cell death.[3] However, the triggers for the induction of autophagy and apoptosis and their roles remain unclear.

In our previous studies, novel glycans consisting of a series of sugar cholestanols were chemically synthesized and evaluated as anticancer drugs in both in vitro and in vivo experiments.[8,14,15] In this study, the expression levels of a series of molecules related to programmed cell death (apoptosis and autophagy) were investigated in glioblastoma cells treated with the same sugar cholestanols. We used CGNH-type glioblastoma cells, cell lines showing epithelial morphology and adhesive capacity. These cell lines possess glial fibrillary acidic protein, vimentin, A2B5, O4, and myelin basic protein.[42] The mRNAs for the glutamate-AMPA receptors (GluR1 and GluR4) were analyzed in CGNH cells using reverse transcriptase–polymerase chain reaction; the cells expressed GluR1 and GluR4.[20] As previously described, these cell lines have the same profile as that of the primary glioblastoma cells de novo.

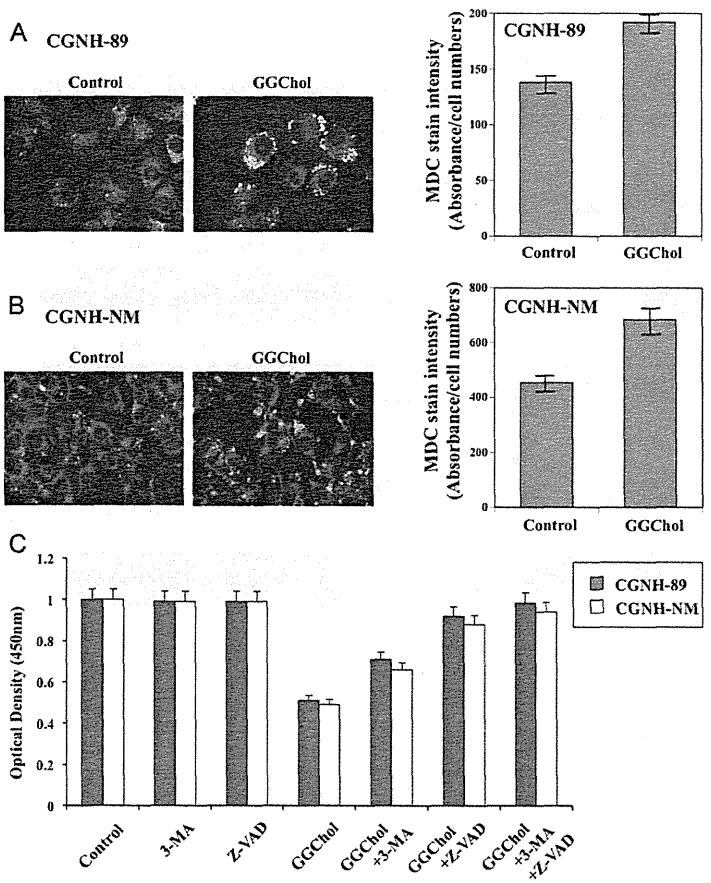

FIG. 4. Fluorescence microscope images showing induction of autophagic cell death in CGNH-89 (**A**) and CGNH-NM (**B**) cells. Original magnification ×200. Bar graph (**C**) demonstrates cell viability in the glioblastoma cells treated with GGChol measured in the presence of antiapoptosis and antiautophagy reagents. Monodansylcadaverine incorporation was quantified and presented as the fold increase ± SEM compared with the control (bar graph, *upper right*). The figures and values are from 3 independent experiments.

In glioblastoma cells treated with sugar cholestanols, the activation of the initiator caspases (extrinsic caspase-8 and intrinsic caspase-9) followed by the activation of the executor caspase (caspase-3) occurred in the glioblastoma cells after treatment with sugar cholestanols. Accordingly, the activation of the cascade involving such caspases induced PARP cleavage, resulting in nuclear fragmentation. Furthermore, the induction of the apoptosis signaling pathway in glioblastoma cells treated with sugar cholestanols appeared to suppress the expression of Bcl-xL and to enhance the expression of Bax in antiapoptotic and proapoptotic manners, respectively. Therefore, the induction of apoptosis appeared to be caused by the disruption of a balance between these anti- and proapoptotic molecules, as described previously.[8,14,15]

One of the most important survival-signaling pathways is mediated by PI3K and its downstream targets, such as Akt and mTOR.[29] Recently, Akt was reported to play an important role in determining the chemosensitivity of many types of cells.[7,10,35] The induction of autophagy requires the activation of Beclin-1 and its interacting partner, Class III PI3K, resulting in the generation of phosphatidylinositol-3′phosphates. This induction is negatively regulated by Class I PI3K via the Akt/mTOR pathway.[41,44,46] In contrast, Beclin-1, a mammalian homolog of the yeast autophagy-related gene Atg6, was observed to be

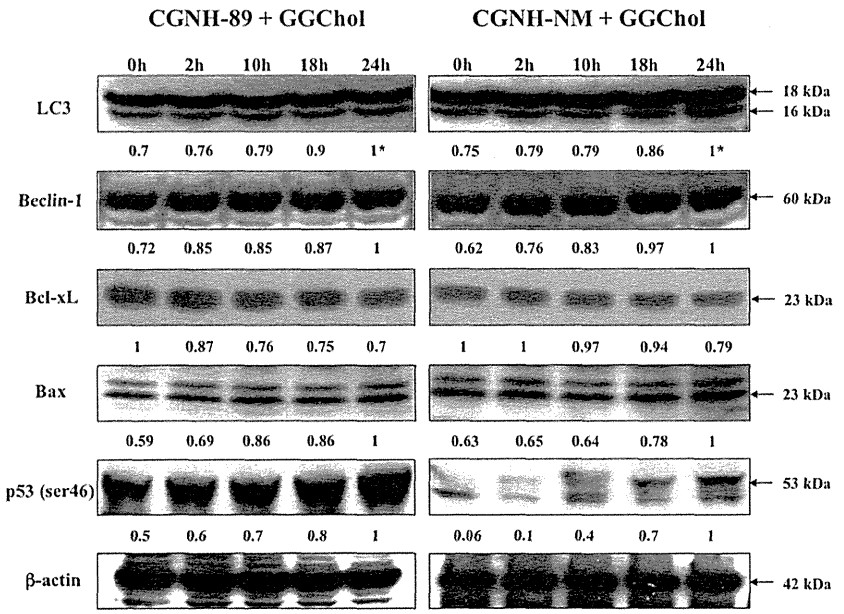

FIG. 5. Western blot analysis in the glioblastoma cells treated with GGChol. Changes in the expression of the autophagy activation, Bcl-2 family members, p53 (ser46) in the CGNH-89 and CGNH-NM cells are shown. The cells were treated with 30 μM of GGChol for 24 hours, and values given below each figure indicate the calculation of each band, and the LC3 active form band (16 kDa), after normalization of their expression to that of β-actin, shown as a percentage compared with the control. There was a significant increase in the active form of LC3 (16 kDa) measured using densitometric analysis.

deleted in breast and prostate cancer cells, and its expression was shown to induce autophagy and inhibit tumorigenicity in MCF-7 breast cancer cells.[27] Furthermore, the microtubule associated protein 1 light chain 3, designated as LC3, exists in 2 forms, which are LC3-I and LC3-II, located in the cytosol and autophagosomal membranes, respectively. LC3 is the first protein that was reported to specifically localize to autophagosome membranes and was later designated as LC3-II (16 kDa), the inner limiting membrane of the autophagosome. During the process of autophagy, cleaved LC3-I conjugates with phosphatidylethanolamine to form LC3-II, which is an important step for autophagosome formation.[25] Immunofluorescence staining of endogenous LC3 can detect autophagy (Fig. 4). The expression of Beclin-1 in glioblastoma cells was slightly increased after treatment with sugar cholestanols along with the decreased expression of the members of the Akt/mTOR pathway. In addition, LC3-II expression was increased, and this hallmark could be used to estimate the abundance of autophagosomes before they are destroyed via fusion with lysosomes.

Recently, p53 has also been revealed to activate autophagy.[22] Several groups have reported the localization of p53 to the outer layer of the mitochondrial membrane and the activation of apoptosis through direct binding to the Bcl-2 family members Bax, Bak, or Bcl-xL.[5,30] The overexpression of p53 was also reported to increase Bax expression in several cell types following the induction of apoptosis.[31,43] The binding of p53 to p53AIP1, which appears to be important for the apoptotic response, is selectively enhanced by the phosphorylation of ser46.[37] We also observed that, in fact, p53 at ser46 was increased in glioblastoma cells after treatment with sugar cholestanols. In addition, the stimulation of cell death controlled by apoptosis and/or at least partially by autophagy was observed in glioblastoma cells treated with sugar cholestanols and cotreated with inhibitors of caspases and autophagy. Therefore, we provided evidence that sugar cholestanols induced apoptosis and autophagic cell death in the same glioblastoma cells. The occurrence of cell death induced by apoptosis was also observed in colorectal cancer cells treated with the same sugar cholestanols (S. Yazawa et al., unpublished observation, 2008).

The mechanism of drug-induced cell death has been accepted to be governed not only by the upregulation of proapoptotic, proautophagic factors or tumor suppressors, but also by the modulation of the survival-signaling pathways.[11] As we previously showed, CGNH cells express Ca^{2+}-permeable AMPA receptors assembled mainly from the GluR1 and/or GluR4 subunits, which contribute to the

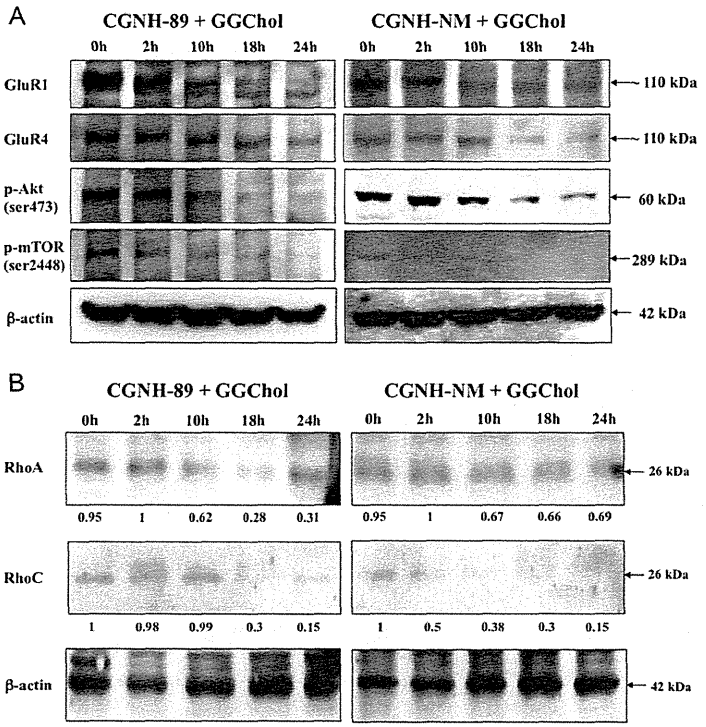

FIG. 6. Western blot analysis of glioblastoma cells treated with GGChol. Changes in the expression levels of the glutamate receptors (GluR1 and GluR4), p-Akt, and p-mTOR **(A)** and Rho GTPases **(B)** in the CGNH-89 and CGNH-NM cells are shown. The CGNH cells were treated with 30 μM of GGChol for 24 hours. The values given below the Rho GTPase figures indicate the calculation of each band after normalization of the expression to that of β-actin, shown as a percentage compared with the control.

invasive and aggressive behavior of glioblastoma.[20] Cell growth appeared to be suppressed in cancer cells treated with the sugar cholestanols, particularly through the activation of the Akt/mTOR pathway (A. Faried et al., unpublished observation, 2009). As reported previously, there is an important survival-signaling pathway that is mediated by the Akt/mTOR pathway[29] and its upstream target, the AMPA receptors.[21]

Our results demonstrated that the sugar cholestanols inhibit the activation of the Akt/mTOR pathway, as shown by the downregulation of phosphorylated Akt at ser473 and phosphorylated mTOR at ser2448. Therefore, we analyzed the expression of the glutamate-AMPA receptors as an upstream target of Akt/mTOR in glioblastoma cells. As expected, we found that the sugar cholestanols inhibited the activation of the glutamate-AMPA receptors, GluR1 and GluR4, in both glioblastoma cell types tested. Taken together, our results suggest that the activation of the glutamate-AMPA receptors–Akt/mTOR pathway was downregulated after treatment with sugar cholestanols.

Ca^{2+}-permeable AMPA receptors and Rho GTPase family members facilitate the migration ability of human glioblastomas.[20,47] In addition, we also evaluated the expression of Rho GTPases (RhoA and RhoC) because they were reported to be related to the degree of malignancy in glioblastoma.[28,47] Furthermore, the inhibition of Rho GTPase signaling has been reported to decrease glioblastoma cell migration.[28] In this study, we showed that the expression of both RhoA and RhoC was decreased after treatment with the sugar cholestanols in a time-dependent manner. Overall, our results showed that different processes of cell death were induced by the sugar cholestanols and that the survival, proliferation, or metastatic properties of glioblastoma cells were affected by some other oncogenic factors (Fig. 8).

Our in vivo experiment using nude mice showed that the sugar cholestanols suppressed tumor growth of CGNH-89 cells that were injected into subcutaneous tissue, possessing the features of human glioblastomas in terms of histological tissue organization. This experiment may provide a reliable in vivo model for studying the response of human glioblastomas to our potential synthetic

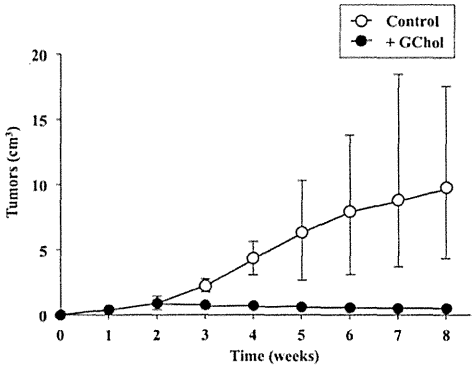

FIG. 7. Line graph showing the anticancer effect of sugar cholestanols on the subcutaneously formed tumors with glioblastoma cells. CGNH-89 cells (2×10^7 cells) were subcutaneously injected into nude mice. Injections of 120 μl of GChol or phosphate-buffered saline only (as a control) were administered intratumorally 3 times (at 14, 15, and 16 days). The values of tumor volumes given indicate the mean ± SD of 5 mice in each group.

glycans (sugar cholestanols). The sugar cholestanol injections reduced the incidence of intratumoral bleeding in the treated mice compared with the untreated mice, accompanied by the suppression of tumor growth and induction of apoptosis. These results indicate that programmed cell death controlled by apoptosis and/or at least partially by autophagy in CGNH cells was stimulated by treatment with our novel synthetic glycans (sugar cholestanols). It remains to be seen whether the sugar cholestanols could be applicable to an in vivo experiment using an intracranial glioma model to investigate their usefulness in chemotherapy against the expected blood-brain barrier.

Conclusions

The activation of programmed cell death in human malignant brain tumor cells induced by treatment with the sugar cholestanols may be involved in not only apoptosis, as we previously demonstrated in several tumor cell lines, but also autophagy, which was demonstrated here for the first time. The sugar cholestanols represent potential pharmaceutical agents against glioblastoma cells.

Disclosure

This work was supported partly by the 21st Century COE

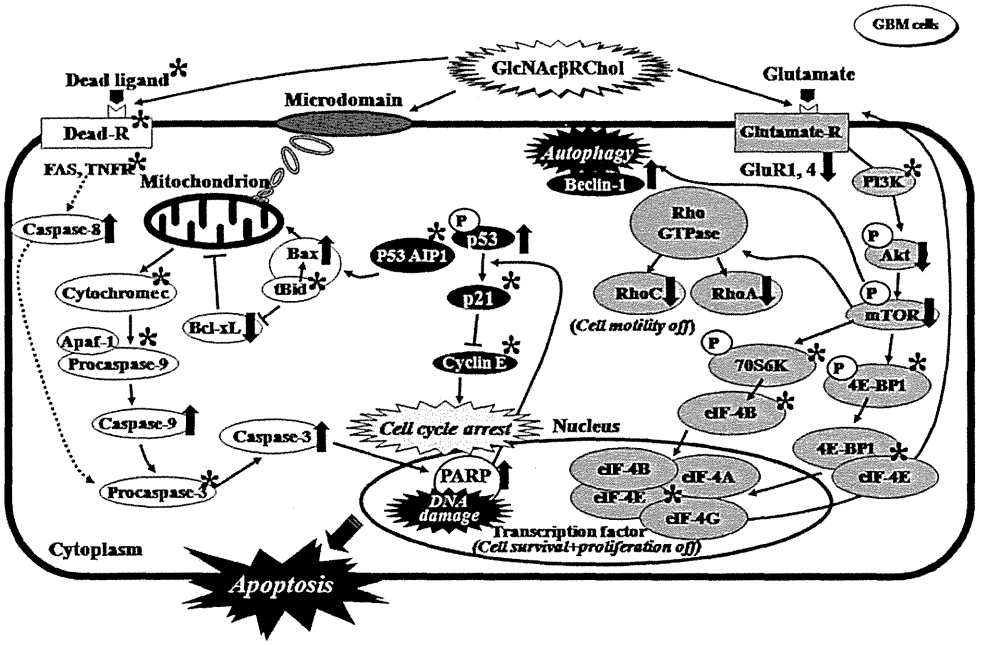

FIG. 8. The predicted effects of sugar cholestanols on cell death inducing both apoptosis and autophagy in the glioblastoma cells resulting from continuous activations and/or suppressions in the expressions of their related molecules. Molecules flagged with an *asterisk* were not examined in this study, but their details have been described in our previous studies.[8–10,14,15,21] TNFR = tumor necrosis factor receptor.

Program, Japan; the Japan Society for the Promotion of Science; and a research grant for collaboration research to Dr. Faried from the Faculty of Medicine at Universitas Padjadjaran.

Author contributions to the study and manuscript preparation include the following. Conception and design: Faried, Arifin, Yazawa. Acquisition of data: Faried, Yazawa. Analysis and interpretation of data: Faried, Yazawa. Drafting the article: Faried, Yazawa. Critically revising the article: all authors. Reviewed submitted version of manuscript: all authors. Approved the final version of the manuscript on behalf of all authors: Faried.

References

1. Biederbick A, Kern HF, Elsässer HP: Monodansylcadaverine (MDC) is a specific in vivo marker for autophagic vacuoles. **Eur J Cell Biol 66:**3–14, 1995
2. Bower M, Newlands ES, Bleehen NM, Brada M, Begent RJ, Calvert H, et al: Multicentre CRC phase II trial of temozolomide in recurrent or progressive high-grade glioma. **Cancer Chemother Pharmacol 40:**484–488, 1997
3. Bursch W, Ellinger A, Gerner C, Fröhwein U, Schulte-Hermann R: Programmed cell death (PCD). Apoptosis, autophagic PCD, or others? **Ann N Y Acad Sci 926:**1–12, 2000
4. Chamberlain MC, Kormanik PA: Practical guidelines for the treatment of malignant gliomas. **West J Med 168:**114–120, 1998
5. Chipuk JE, Kuwana T, Bouchier-Hayes L, Droin NM, Newmeyer DD, Schuler MM, et al: Direct activation of Bax by p53 mediates mitochondrial membrane permeabilization and apoptosis. **Science 303:**1010–1014, 2004
6. Edinger AL, Thompson CB: Death by design: apoptosis, necrosis and autophagy. **Curr Opin Cell Biol 16:**663–669, 2004
7. Fahy BN, Schlieman MG, Virudachalam S, Bold RJ: Inhibition of AKT abrogates chemotherapy-induced NF-kappaB survival mechanisms: implications for therapy in pancreatic cancer. **J Am Coll Surg 198:**591–599, 2004
8. Faried A, Faried LS, Nakagawa T, Yamauchi T, Kitani M, Sasabe H, et al: Chemically synthesized sugar-cholestanols possess a preferential anticancer activity involving promising therapeutic potential against human esophageal cancer. **Cancer Sci 98:**1358–1367, 2007
9. Faried A, Faried LS, Usman N, Kato H, Kuwano H: Clinical and prognostic significance of RhoA and RhoC gene expression in esophageal squamous cell carcinoma. **Ann Surg Oncol 14:**3593–3601, 2007
10. Faried LS, Faried A, Kanuma T, Nakazato T, Tamura T, Kuwano H, et al: Inhibition of the mammalian target of rapamycin (mTOR) by rapamycin increases chemosensitivity of CaSki cells to paclitaxel. **Eur J Cancer 42:**934–947, 2006
11. Fraser M, Leung B, Jahani-Asl A, Yan X, Thompson WE, Tsang BK: Chemoresistance in human ovarian cancer: the role of apoptotic regulators. **Reprod Biol Endocrinol 1:**66, 2003
12. Fritz G, Just I, Kaina B: Rho GTPases are over-expressed in human tumors. **Int J Cancer 81:**682–687, 1999
13. Goto J, Suzaki K, Nambara T: Synthesis of conjugated cholesterol and cholestanols. **Chem Pharm Bull (Tokyo) 27:**1926–1931, 1979
14. Hashimoto S, Tsuboi K, Asao T, Kuwano H, Nishimura T, Nakagawa T, et al: Anti-tumor effect of chemically synthesized novel glycoconjugates. **Glycoconj J 22:**311, 2005
15. Hahismoto S, Yazawa S, Asao T, Faried A, Nishimura T, Tsuboi K, et al: Novel sugar-cholestanols as anticancer agents against peritoneal dissemination of tumor cells. **Glycoconj J 25:**531–544, 2008
16. Hoelzinger DB, Mariani L, Weis J, Woyke T, Berens TJ, McDonough WS, et al: Gene expression profile of glioblastoma multiforme invasive phenotype points to new therapeutic targets. **Neoplasia 7:**7–16, 2005
17. Hoorens A, Van de Casteele M, Klöppel G, Pipeleers D: Glucose promotes survival of rat pancreatic beta cells by activating synthesis of proteins which suppress a constitutive apoptotic program. **J Clin Invest 98:**1568–1574, 1996
18. Horiuchi A, Imai T, Wang C, Ohira S, Feng Y, Nikaido T, et al: Up-regulation of small GTPases, RhoA and RhoC, is associated with tumor progression in ovarian carcinoma. **Lab Invest 83:**861–870, 2003
19. Ishiuchi S, Nakazato Y, Iino M, Ozawa S, Tamura M, Ohye C: In vitro neuronal and glial production and differentiation of human central neurocytoma cells. **J Neurosci Res 51:**526–535, 1998
20. Ishiuchi S, Tsuzuki K, Yoshida Y, Yamada N, Hagimura N, Okado H, et al: Blockage of $Ca^{(2+)}$-permeable AMPA receptors suppresses migration and induces apoptosis in human glioblastoma cells. **Nat Med 8:**971–978, 2002
21. Ishiuchi S, Yoshida Y, Sugawara K, Aihara M, Ohtani T, Watanabe T, et al: Ca^{2+}-permeable AMPA receptors regulate growth of human glioblastoma via Akt activation. **J Neurosci 27:**7987–8001, 2007
22. Jin S: p53, autophagy and tumor suppression. **Autophagy 1:**171–173, 2005
23. Kamai T, Tsujii T, Arai K, Takagi K, Asami H, Ito Y, et al: Significant association of Rho/ROCK pathway with invasion and metastasis of bladder cancer. **Clin Cancer Res 9:**2632–2641, 2003
24. Kanzawa T, Germano IM, Komata T, Ito H, Kondo Y, Kondo S: Role of autophagy in temozolomide-induced cytotoxicity for malignant glioma cells. **Cell Death Differ 11:**448–457, 2004
25. Kondo Y, Kanzawa T, Sawaya R, Kondo S: The role of autophagy in cancer development and response to therapy. **Nat Rev Cancer 5:**726–734, 2005
26. Lefranc F, Brotchi J, Kiss R: Possible future issues in the treatment of glioblastomas: special emphasis on cell migration and the resistance of migrating glioblastoma cells to apoptosis. **J Clin Oncol 23:**2411–2422, 2005
27. Liang XH, Jackson S, Seaman M, Brown K, Kempkes B, Hibshoosh H, et al: Induction of autophagy and inhibition of tumorigenesis by beclin 1. **Nature 402:**672–676, 1999
28. Manning TJ Jr, Parker JC, Sontheimer H: Role of lysophosphatidic acid and rho in glioma cell motility. **Cell Motil Cytoskeleton 45:**185–199, 2000
29. McCormick F: Cancer: survival pathways meet their end. **Nature 428:**267–269, 2004
30. Mihara M, Erster S, Zaika A, Petrenko O, Chittenden T, Pancoska P, et al: p53 has a direct apoptogenic role at the mitochondria. **Mol Cell 11:**577–590, 2003
31. Miyashita T, Krajewski S, Krajewska M, Wang HG, Lin HK, Liebermann DA, et al: Tumor suppressor p53 is a regulator of bcl-2 and bax gene expression in vitro and in vivo. **Oncogene 9:**1799–1805, 1994
32. Munafó DB, Colombo MI: A novel assay to study autophagy: regulation of autophagosome vacuole size by amino acid deprivation. **J Cell Sci 114:**3619–3629, 2001
33. Nelson DA, White E: Exploiting different ways to die. **Genes Dev 18:**1223–1226, 2004
34. Newton HB: Small-molecule and antibody approaches to molecular chemotherapy of primary brain tumors. **Curr Opin Investig Drugs 8:**1009–1021, 2007
35. Nguyen DM, Chen GA, Reddy R, Tsai W, Schrump WD, Cole G Jr, et al: Potentiation of paclitaxel cytotoxicity in lung and esophageal cancer cells by pharmacologic inhibition of the phosphoinositide 3-kinase/protein kinase B (Akt)-mediated signaling pathway. **J Thorac Cardiovasc Surg 127:**365–375, 2004
36. Nichols WW, Murphy DG, Cristofalo VJ, Toji LH, Greene AE, Dwight SA: Characterization of a new human diploid cell strain, IMR-90. **Science 196:**60–63, 1977
37. Oda K, Arakawa H, Tanaka T, Matsuda K, Tanikawa C, Mori T, et al: p53AIP1, a potential mediator of p53-dependent apop-

tosis, and its regulation by Ser-46-phosphorylated p53. **Cell 102:**849–862, 2000
38. Ogier-Denis E, Codogno P: Autophagy: a barrier or an adaptive response to cancer. **Biochim Biophys Acta 1603:**113–128, 2003
39. Osaki M, Oshimura M, Ito H: PI3K-Akt pathway: its functions and alterations in human cancer. **Apoptosis 9:**667–676, 2004
40. Paglin S, Hollister T, Delohery T, Hackett N, McMahill M, Sphicas E, et al: A novel response of cancer cells to radiation involves autophagy and formation of acidic vesicles. **Cancer Res 61:**439–444, 2001
41. Petiot A, Ogier-Denis E, Blommaart EF, Meijer AJ, Codogno P: Distinct classes of phosphatidylinositol 3'-kinases are involved in signaling pathways that control macroautophagy in HT-29 cells. **J Biol Chem 275:**992–998, 2000
42. Sasaki A, Tamura M, Hasegawa M, Ishiuchi S, Hirato J, Nakazato Y: Expression of interleukin-1beta mRNA and protein in human gliomas assessed by RT-PCR and immunohistochemistry. **J Neuropathol Exp Neurol 57:**653–663, 1998
43. Selvakumaran M, Lin HK, Miyashita T, Wang HG, Krajewski S, Reed JC, et al: Immediate early up-regulation of bax expression by p53 but not TGF beta 1: a paradigm for distinct apoptotic pathways. **Oncogene 9:**1791–1798, 1994
44. Shintani T, Klionsky DJ: Autophagy in health and disease: a double-edged sword. **Science 306:**990–995, 2004
45. Stupp R, Mason WP, van den Bent MJ, Weller M, Fisher B, Taphoorn MJ, et al: Radiotherapy plus concomitant and adjuvant temozolomide for glioblastoma. **N Engl J Med 352:**987–996, 2005
46. Wang CW, Klionsky DJ: The molecular mechanism of autophagy. **Mol Med 9:**65–76, 2003
47. Yan B, Chour HH, Peh BK, Lim C, Salto-Tellez M: RhoA protein expression correlates positively with degree of malignancy in astrocytomas. **Neurosci Lett 407:**124–126, 2006
48. Yung WK, Prados MD, Yaya-Tur R, Rosenfeld SS, Brada M, Friedman HS, et al: Multicenter phase II trial of temozolomide in patients with anaplastic astrocytoma or anaplastic oligoastrocytoma at first relapse. **J Clin Oncol 17:**2762–2771, 1999

Manuscript submitted July 16, 2013.
Accepted January 23, 2014.
Please include this information when citing this paper: published online March 28, 2014; DOI: 10.3171/2014.1.JNS131534.
Address correspondence to: Ahmad Faried, M.D., Ph.D., Department of Neurosurgery, Faculty of Medicine, Universitas Padjadjaran–Dr. Hasan Sadikin Hospital, Jl. Pasteur No. 38, Bandung, West Java 40161, Indonesia. email: faried.fkup@gmail.com.

Gen Thorac Cardiovasc Surg (2014) 62:308–313
DOI 10.1007/s11748-014-0375-0

ORIGINAL ARTICLE

Risk assessment of perioperative mortality after pulmonary resection in patients with primary lung cancer: the 30- or 90-day mortality

Kenji Tomizawa · Noriyasu Usami · Koichi Fukumoto · Noriaki Sakakura · Takayuki Fukui · Simon Ito · Shunzo Hatooka · Hiroyuki Kuwano · Tetsuya Mitsudomi · Yukinori Sakao

Received: 21 November 2013 / Accepted: 14 January 2014 / Published online: 13 February 2014

Abstract
Objectives Although 30-day mortality rate is adapted to evaluate perioperative mortality after surgery, whether 90-day mortality rate adequately evaluates perioperative mortality remains unknown. Therefore, we analyzed 30- and 90-day mortality rates after pulmonary resection in patients with primary lung cancer.
Methods A total of 2207 pulmonary resections for primary lung cancer performed between 1996 and 2010 at the Aichi Cancer Center Hospital were analyzed and divided into two groups of almost equal number: the early period group (1070 patients, 1996–2004) and the late period group (1137 patients, 2005–2010). Sixty-six and 34 patients died within a year during the early and late periods, respectively. The causes of death (recurrence, bleeding, sudden death, respiratory failure, and adverse event of chemotherapy), and 30- and 90-day mortality rates were investigated.
Results The 30-/90-day mortality rates in the early and late period groups were 0.56/0.75 and 0.35/0.79 %, respectively. The postoperative survival days of 75 patients who died from recurrence within 1 year after pulmonary resection and 7 patients from bleeding or sudden death were more than 91 days and <30 days, respectively. The median postoperative survival of patients who died from respiratory failure was 67 days (range 20–142 days) in the early period and 100 days (range 47–149 days) in the late period. In the late period, it was difficult to assess perioperative mortality of pulmonary complications with 30-day mortality.
Conclusions A risk assessment of perioperative mortality after pulmonary resection should be performed using the 30- and 90-day mortality.

Keywords 30-day mortality · 90-day mortality · Primary lung cancer

The article is based on a study first reported in the Japanese J. Lung Cancer, 2013;53:93–8.

Presented at The 65th Annual Scientific Meeting of The Japanese Association for Thoracic Surgery.

K. Tomizawa · N. Usami · N. Sakakura · Y. Sakao (✉)
Department of Thoracic Surgery, Aichi Cancer Center Hospital, 1-1 Kanokoden, Chikusa-ku, Nagoya, Aichi 464-8681, Japan
e-mail: ysakao@aichi-cc.jp

K. Tomizawa · H. Kuwano
Department of General Surgical Science, Graduate School of Medicine, Gunma University, Maebashi, Japan

N. Usami · K. Fukumoto · T. Fukui
Department of Thoracic Surgery, Nagoya University Graduate School of Medicine, Nagoya, Japan

S. Ito
Department of Thoracic Surgery, Nagoya Daini Red Cross Hospital, Nagoya, Japan

S. Hatooka
Department of Thoracic Surgery, Ichinomiya Nishi Hospital, Ichinomiya, Japan

T. Mitsudomi
Division of Thoracic Surgery, Kinki University Hospital, Higashiosaka, Japan

Introduction

Thirty-day mortality and in-hospital death are important considerations to estimate operative mortality when evaluating the option of surgery for lung cancer as described in the Guideline of British Thoracic Society and the Society

for Cardiothoracic Surgery in Great Britain and Ireland [1]. A fatal case within 30 days after surgery is defined as a direct operative death in the seventh edition of the general rule for clinical and pathological record of lung cancer in the Japan Lung Cancer Society [2], and 30-day mortality patient is defined as one of the surgical safety indices (surgical risk) at a medical facility. In clinical practice, postoperative survival could exceed 30 days with aggressive intensive medical care for postoperative complications, but we often experienced fatal cases in 31 days or more after pulmonary resection. Recently, some reports have occasionally described that not only the 30-day mortality rate but also the 90-day mortality rate are useful as a surgical risk index [3–5]. Bryant et al. [4] reported that the 30- and 90-day mortality rates in 1845 patients were 3.0 and 5.4 %, respectively, with the 90-day mortality rate being approximately twice as high as the 30-day mortality rate. Most reports for the 90-day mortality rate after pulmonary resection for primary lung cancer are presented abroad, and there are only a few reports on the 90-day mortality rate in Japan. In this study, we analyzed the 30- and 90-day mortality rates after pulmonary resection for primary lung cancer in our institution, and then examined their usability for surgical risk assessment.

Methods

A total of 2207 patients with primary lung cancer underwent curative pulmonary resection between January 1996 and December 2010 at the Aichi Cancer Center Hospital. They were retrospectively analyzed and divided into two groups of almost equal number: the early period group (1070 patients, 1996–2004) and the late period group (1137 patients, 2005–2010). Patients who underwent exploratory thoracotomy were excluded. We compared the two groups for sex, smoking history, American Society of Anesthesiologist (ASA) score [6], preoperative forced expiratory volume in one second ($FEV_{1.0}$), surgical procedure, pathological stage, histological findings, neoadjuvant chemotherapy, and platinum-doublet adjuvant chemotherapy. The pathological stage was decided according to the seventh edition of the tumor–node–metastasis (TNM) staging system [7]. The patients who died within a year after pulmonary resection were extracted irrespective of the hospital discharge. The cause of death and the 30-day, 90-day, and 1-year mortality rates were examined and classified into five fatal categories: recurrence, respiratory failure, sudden death, bleeding, and adverse event of chemotherapy. These categories were defined as follows: patients' death due to postoperative recurrence, pneumonia/acute respiratory distress syndrome (ARDS)/empyema, no cause, and circulation failure owing to perioperative hemorrhage were defined as "recurrence," "respiratory failure," "sudden death," and "bleeding," respectively. Furthermore, because postoperative adjuvant chemotherapy was established after 2004 [8] and also actively executed at our hospital, we added adverse event of chemotherapy as one of the five fatal categories. All patients provided a written informed consent on admission. An appropriate and comprehensive approval, including permission for application of personal data in clinical studies, was obtained in advance from our institutional review board. Statistical analysis was performed using the Chi Square test or t test to compare proportions, and the two-sided significance level was set at $p < 0.05$.

Results

Patient characteristics are shown in Table 1. Compared with the early period group, the late period group had more patients aged ≤70 years with lower ASA scores. When the operative procedures in the late period were compared with those in the early period, pneumonectomy and bi-lobectomy were decreased, whereas segmentectomy or less were increased. Neoadjuvant chemotherapy was administered to

Table 1 Clinicopathological characteristics of patients with primary lung cancer in the early and late periods

	Early period (1994–2004) $n = 1070$	Late period (2005–2010) $n = 1137$	p
Age (<70/≥70)	256/814	397/740	<0.0001
Sex (male/female)	416/654	468/669	0.274
Smoking (never/ever)	433/637	485/652	0.297
ASA score (1/2/3/4)	296/722/52/0	380/719/38/0	0.005
% $FEV_{1.0}$ (<70/≥70)	147/923	143/994	0.414
Operation procedure			
Pneumonectomy	44	31	<0.0001
Bi-lobectomy	50	29	
Lobectomy	906	923	
Segmentectomy or less	70	154	
Pathological stage[a] (I/II/III/IV)	612/189/247/22	666/203/250/18	0.761
Histology (AD/non-AD)	776/294	795/341	0.188
Neoadjuvant chemotherapy	44	21	0.0017
Adjuvant chemotherapy (platinum doublet)	3	150	<0.0001

Never smoker, Brinkman Index × 100; ASA score, American Society of Anesthesiologist score; $FEV_{1.0}$, forced expiratory volume in 1 s; AD, adenocarcinoma

[a] According to the tumor–node–metastasis (TNM) classification of malignant tumors, 7th edition